HYPERFINE STRUCTURE IN THE MICROWAVE SPECTRUM OF WATER

I. QUADRUPOLE COUPLING IN DEUTERATED WATER

By D. W. POSENER*

[*Manuscript received January* 2, 1957]

Summary

Measurement of hyperfine structure in the microwave spectrum of D_2O gives $(eqQ)_{OD}=+353\pm4$ kc/s for the quadrupole coupling constant of the deuteron in the direction of the OD bond, and the corresponding electric field gradient is $q_{OD}=\langle\partial^2V/\partial\xi^2\rangle=(1\cdot78\pm0\cdot02)\times10^{15}$ e.s.u.

The observed hyperfine splitting of HDO is not accounted for by a simple quadrupole interaction and appears to require relatively large magnetic interaction terms for a complete description.

I. INTRODUCTION

Deuterium has frequently been used in spectroscopy to assist in structural determinations, but hyperfine splitting arising from the quadrupole moment of the deuteron has been reported in only a few microwave spectra (White 1955*b* ; Weisbaum, Beers, and Herrmann 1955). The very common occurrence of hydrogen in molecules, and the ready availability of deuterium, whose quadrupole moment is known with some accuracy, suggest that a study of such hyperfine splitting can give useful information about many substances.

Partial resolution of deuteron coupling in DCCCl and in DCN has been observed by White (1955*b*) who reported values of $+175\pm20$ kc/s and $\pm290\pm120$ kc/s respectively for the coupling constant eqQ of the deuteron in these molecules. Weisbaum, Beers, and Herrmann (1955) have deduced from the broadening of the $3_{30}\leftarrow3_{31}$ line of HDO that for this molecule eqQ in the bond direction is 272 ± 90 kc/s.

It is apparent then that the small quadrupole moment of the deuteron, $Q=(2\cdot738\pm0\cdot014)\times10^{-27}$ cm^2 (Kolsky *et al.* 1952), and the predominantly spherical electron charge distribution near the nucleus combine to give splittings which are very small (of the order of tens or hundreds of kc/s) compared with those due to, say, the halogens, where the effects may be a thousand times larger. Accordingly, the spectra need to be examined under the highest resolution available.

Hyperfine structure in the deuterated water molecules has now been examined because favourable transitions can be chosen for study and sufficient additional information concerning the molecules is available for the derivation of significant conclusions from the experimental results.

* Division of Electrotechnology, C.S.I.R.O., University Grounds, Chippendale, N.S.W.

It is to be expected that magnetic hyperfine splitting, of the order of a few kc/s, will be noticeable at sufficiently high resolution (White 1955*c*; Okaya 1956), and evidence of such interactions will be given. Analysis of these magnetic effects is omitted in the present work, however, and it is intended to discuss them in a later paper.

II. Experimental

A block diagram of the spectroscope, which will be described more fully elsewhere, is shown in Figure 1.

The $2_{20} \leftarrow 2_{21}$ line of HDO at 10,278 Mc/s (Strandberg 1949) and the $3_{13} \leftarrow 2_{20}$ D_2O transition at 10,919 Mc/s (Beard and Bianco 1952; Posener 1953) were examined, typical spectra being shown in Figures 2 and 3. Because of the low J values involved, the quadrupole splittings are sufficiently large to be reasonably well resolved.

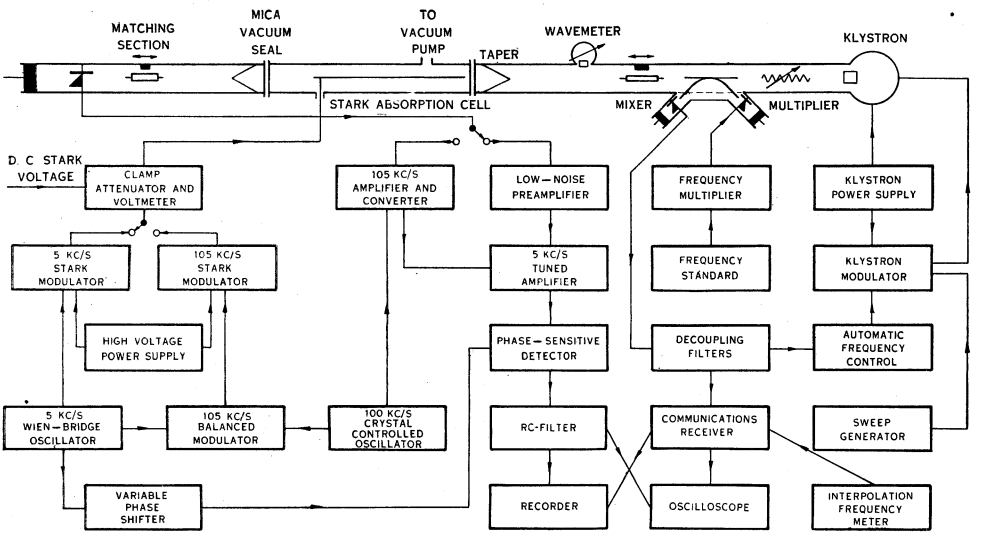

Fig. 1.—Block diagram of the microwave spectroscope.

Square-wave Stark modulation at 5 kc/s, clamped to within a few volts of zero, was employed for detection; the well-known broadening effects of modulation are illustrated in Figure 4, which compares the D_2O transition under conditions which were identical except for modulation frequency and amplifier gain.

In spite of the lightness of the molecules, the Doppler effect is small at the transition frequencies involved, the half-width at half-power being about 12 kc/s at 200 °K. A 12-ft S-band absorption cell was used in order to reduce wall-collision broadening. A contribution of about 7 kc/s to the half half-width due to such broadening was estimated from the experimental results in this and in an X-band cell. The large cell cross section enabled an adequate signal-to-noise ratio to be obtained at a power level (a few microwatts) well below that necessary to cause observable saturation effects to occur. At the dry-ice

temperature at which the cell was operated the vapour pressure of water is of the order of 0·5 μ Hg, and this would give rise to about 7 kc/s of pressure broadening.

Control of the pressure was in fact difficult; the cell was not rigorously at dry-ice temperature because of the large heat flow in from the ends, and a 5°

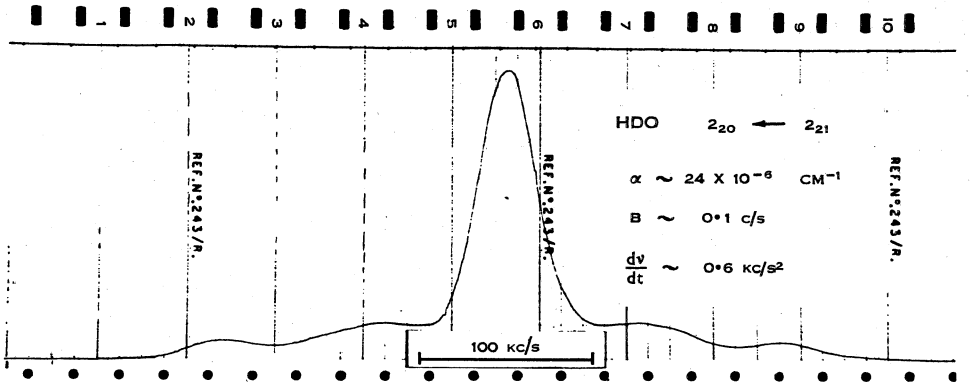

Fig. 2.—Recording of the HDO spectrum.

rise in temperature could double the vapour pressure (Hilsenrath *et al.* 1955). Apart from condensed water, absorption on the internal surfaces of the cell complicated the equilibrium conditions. Highest resolution was obtained during continuous pumping of the sample, and thus optimum experimental conditions were not readily reproducible.

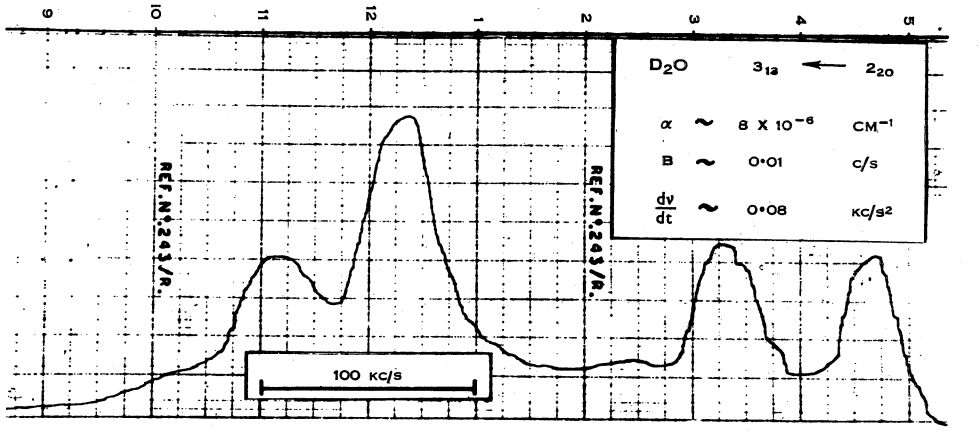

Fig. 3.—Recording of the D_2O spectrum.

Adhesive polythene tape was used between waveguide coupling flanges far from the cell itself to reduce the amount of atmospheric water vapour condensing on the cell mica windows, but a slow accumulation of ice occurred and had to be periodically removed to prevent mismatch conditions arising in the oversize guide, due apparently to the excitation of higher modes.

The signal strength was weak at the low pressure and low microwave power used, and it was necessary to critically select crystals for their detector performance. From several dozen crystals of different types available the best results were obtained with a British Thomson-Houston CS4-B coaxial type crystal chosen from a number which had repeatedly had their tungsten whiskers resharpened and new contacts made with the silicon block, and which then were tested under operating conditions.

In this microwave region a Varian X-13 klystron was used as a source. Frequency control, sweep, and measurement essentially followed the methods described by Lee *et al.* (1953) and by White (1955*a*). In the present equipment the f.m. receiver was specially built for high i.f. gain, and included across the main tuning circuit a small capacitor consisting of two opposed semicircular

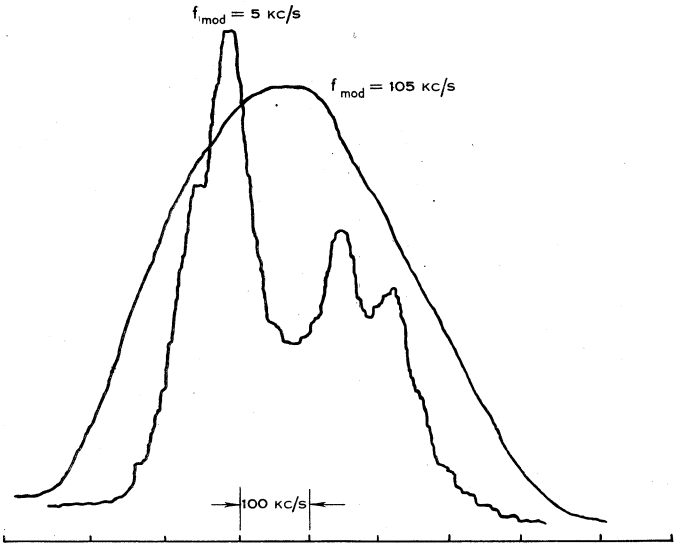

Fig. 4.—The D_2O spectrum showing loss of resolution at high modulation frequency.

plates, whose relative rotation by means of a synchronous motor controlled the microwave sweep; a full revolution provided two sweeps in opposite directions and permitted the effects of time delays in the detector filters to be averaged out.

The frequency standard itself is a nominal 100 kc/s quartz oscillator forming part of the Australian standard of frequency, and is constantly compared with other oscillators, with international radio time signals, and with astronomical time. The frequency is accurate to better than 2 parts in 10^8 at all times. Because of the high multiplication factor, phase instability in the standard oscillator prevented the attainment of a really clean audio beat in the a.m. receiver, although the zero of the note could generally be determined to better than 1 kc/s. In sweeping through a spectrum the zero beat was detected audibly, and frequency markers at about 20 kc/s intervals placed on the chart with an operations pen. The sweep was sufficiently linear to allow of frequency determination to 1 kc/s.

Filter noise-power bandwidths B of approximately 0·1 c/s and 0·01 c/s were used, with sweep rates $d\nu/dt$ of approximately 1 kc/s^2 and 0·1 kc/s^2, respectively, small enough to prevent significant distortion (Brodersen 1953; Smith 1955). With the narrowest bandwidth, such as used to obtain Figure 3, the sweep time was too long (about 2 hr in each direction) for continuous pumping of the cell to be employed, and thus the highest resolution was not reached; the broader filter was used to obtain the results of Figures 2, 5, 6, and 7, and allowed improved resolution at the expense of signal-to-noise ratio.

TABLE 1
HDO QUADRUPOLAR ENERGY SPLITTINGS

F	Rotational Energy Level	
	2_{20}	2_{21}
1	$0{\cdot}2685\chi_{aa}+0{\cdot}0423\chi_{bb}$	$0{\cdot}25\chi_{aa}$
2	$-0{\cdot}2685\chi_{aa}-0{\cdot}0423\chi_{bb}$	$-0{\cdot}25\chi_{aa}$
3	$0{\cdot}0767\chi_{aa}+0{\cdot}0121\chi_{bb}$	$0{\cdot}0714\chi_{aa}$

TABLE 2
D_2O QUADRUPOLAR ENERGY SPLITTINGS

F	ε	Rotational Energy Level	
		3_{13}	2_{20}
0	2		$0{\cdot}55099\chi_{aa}+0{\cdot}12609\chi_{bb}$
1	2	$-0{\cdot}51140\chi_{aa}-0{\cdot}42797\chi_{bb}$	$0{\cdot}27549\chi_{aa}+0{\cdot}06304\chi_{bb}$
2	0		$0{\cdot}36164\chi_{aa}+0{\cdot}08276\chi_{bb}$
	2	$-0{\cdot}12785\chi_{aa}-0{\cdot}10699\chi_{bb}$	$-0{\cdot}47970\chi_{aa}-0{\cdot}10978\chi_{bb}$
3	0	$-0{\cdot}36413\chi_{aa}-0{\cdot}30473\chi_{bb}$	
	2	$0{\cdot}59853\chi_{aa}+0{\cdot}50088\chi_{bb}$	$-0{\cdot}31485\chi_{aa}-0{\cdot}07205\chi_{bb}$
4	2	$0{\cdot}31963\chi_{aa}+0{\cdot}26748\chi_{bb}$	$0{\cdot}15743\chi_{aa}+0{\cdot}03603\chi_{bb}$
5	2	$-0{\cdot}21309\chi_{aa}-0{\cdot}17832\chi_{bb}$	

III. THEORY

The problem of a single quadrupolar nucleus in an asymmetric rotor molecule is well known (Strandberg 1954, Ch. IV), and for HDO, using $\varkappa=-0{\cdot}6841$ (Posener and Strandberg 1954), the quadrupolar energy splittings ΔW and the relative intensities of transitions between these levels are listed in Tables 1 and 5 respectively, in which $\chi_{ij}=eQV_{ij}$, and i and j refer to the principal inertial axes of the molecule.

Robinson and Cornwell (1953) have discussed the case of two quadrupolar nuclei, and the hyperfine energies for D_2O, labelled according to their notation,

TABLE 3

FIELD GRADIENT TENSOR RELATIONS FOR ASSUMPTION OF CYLINDRICAL SYMMETRY

	HDO	D_2O
V_{aa}	$0{\cdot}87698q_{OD}$	$0{\cdot}43715q_{OD}$
V_{bb}	$-0{\cdot}37698q_{OD}$	$0{\cdot}06285q_{OD}$

are given in Table 2, with the corresponding relative intensities in Table 4; we have used $\varkappa = -0{\cdot}5423$ (Posener 1953; Benedict, Gailar, and Plyler 1956).

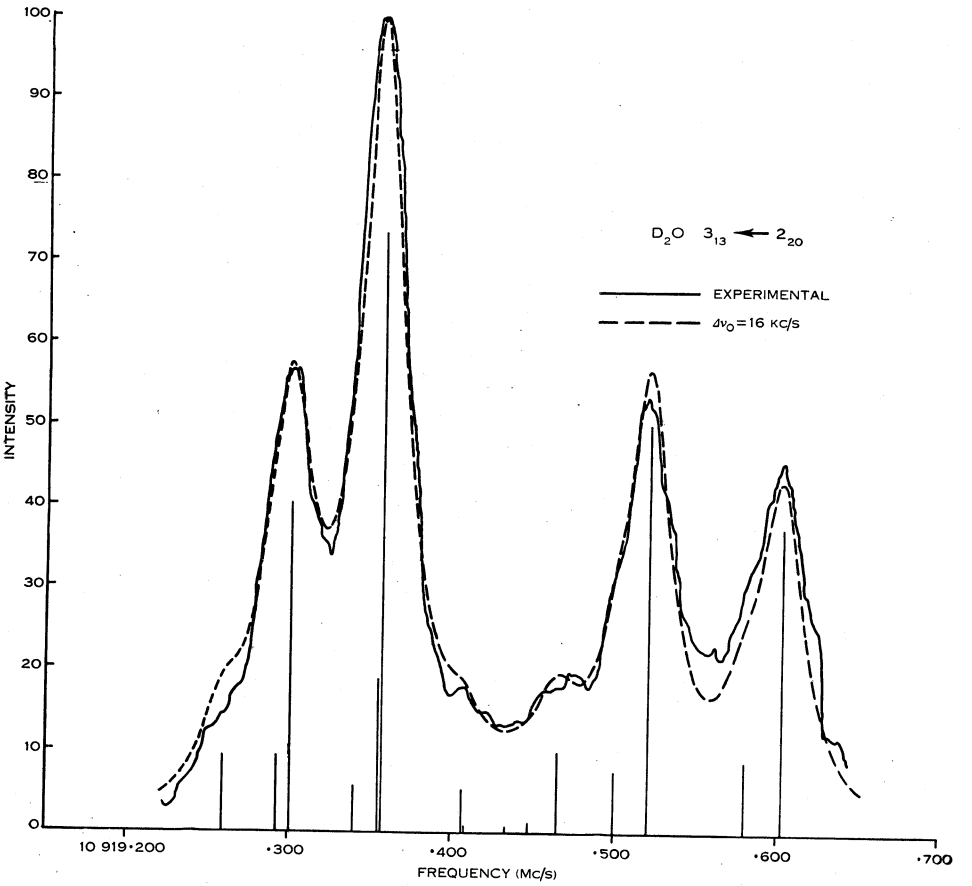

Fig. 5.—Comparison of trial frequencies and observed spectrum in D_2O.

In D_2O the χ_{ij} have not the same values as in HDO, because of the different principal axes of the two molecules. If the χ_{ij} were known sufficiently accurately for both molecules it would be possible to determine the principal axes of the field gradient tensor in terms of the molecular geometry. This accuracy is not

reached in the present work, and in fact it is convenient to make the simplifying assumption (Weisbaum, Beers, and Herrmann 1955) that the field gradient tensor V_{ij} is cylindrically symmetric about the OD bond axis, which then becomes a principal axis of this tensor. If we call this direction ξ, then a simple transformation gives the V_{ij} in terms of the single parameter $V_{\xi\xi}=\langle\partial^2 V/\partial\xi^2\rangle=q_{\mathrm{OD}}$ say, and we get the numerical results of Table 3. Since the electronic structure of the molecules is not affected by isotopic substitution, at least to this approximation, q_{OD} should be the same for both HDO and D_2O.

Thus the transition frequencies of the hyperfine splitting can be written in the form

$$\nu=\nu_0+A\chi_{aa}+B\chi_{bb}, \quad \ldots\ldots\ldots\ldots\ldots\ldots \quad (1)$$

where ν_0 is the " unperturbed " transition frequency and A and B are calculable constants ; or, to the approximation discussed above,

$$\nu=\nu_0+C(eqQ)_{\mathrm{OD}}. \quad \ldots\ldots\ldots\ldots\ldots\ldots \quad (2)$$

TABLE 4

D_2O $3_{13}\leftarrow 2_{20}$ HYPERFINE STRUCTURE

Transition F'	$\varepsilon'\leftarrow F''$		ε''	Measured Frequency (Mc/s) (*a*)	Trial Frequency (Mc/s) (*b*)	Calculated Frequency (Mc/s) (*c*)*	(*d*)†	Relative Intensity (Calculated)
1	2	0	2		10,919·260	10,919·249	10,919·244	12·73
1	2	1	2		·293	·274	·288	12·73
3	0	2	0	10,919·301±0·001	·301	·301	·299	54·96
2	2	2	0		·340	·356	·340	7·82
2	2	1	2		·355	·364	·354	25·45
5	2	4	2	10,919·357±0·001	·357	·355	·358	100·00
3	0	3	2		·407	·362	·407	7·22
1	2	2	2		·408	·343	·408	1·04
3	0	2	2		·434	·377	·434	1·12
2	2	3	2		·448	·418	·448	1·82
4	2	4	2		·465	·479	·450	13·64
2	2	2	2		·500	·433	·474	10·37
4	2	3	2	10,919·521±0·001	·521	·522	·525	68·18
3	2	3	2		·580	·587	·574	11·87
3	2	2	2	10,919·603±0·001	·603	·602	·600	51·12
1	2	2	0	not considered				0·78
3	0	4	2	not considered				0·34
3	2	2	0	not considered				0·08
3	2	4	2	not considered				0·57

* For $\nu_0=10{,}919{\cdot}419$ Mc/s, $\chi_{aa}=37$ kc/s, $\chi_{bb}=235$ kc/s.

† For $\nu_0=10{,}919{\cdot}420$ Mc/s, $(eqQ)_{\mathrm{OD}}=353$ kc/s.

IV. DISCUSSION

(*a*) *The D_2O Spectrum*

The frequencies of the major transitions in D_2O (Fig. 3) were determined by obtaining approximate parameters from equation (**2**), synthesizing a theoretical curve for the whole group of transitions, comparing this with the

observed spectrum, and then by appropriate adjustment of the more significant transition frequencies obtaining the best agreement. This is shown in Figure 5. The trial curve was computed for the frequencies listed in column (*b*) of Table 4, using a half half-width $\Delta\nu_0=16$ kc/s and a Lorentz line shape; it is probable that, because of the relatively large Doppler contribution to the broadening, there would actually be a considerable Gaussian character involved, but inclusion

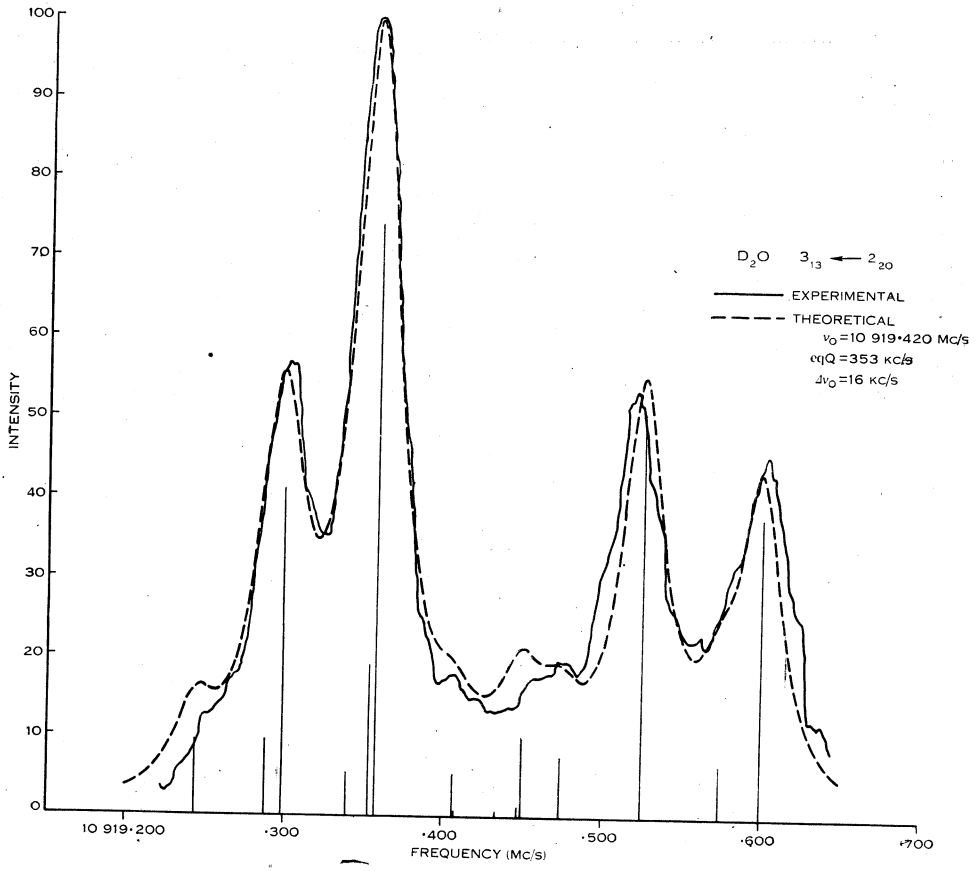

Fig. 6.—Calculated and observed spectra of D_2O.

of this refinement did not seem justified at the present stage. It is of interest that the best resolution obtainable in a 15-ft *X*-band cell gave a $\Delta\nu_0$ of the order of 25 kc/s.

The four largest components reasonably resolved in Figure 5 give frequencies (listed in column (*a*) of Table 4) which can be put into the set of equations like (**2**) to give a least squares solution $\nu_0=10{,}919\cdot419\pm0\cdot001$ Mc/s, $\chi_{aa}=37\pm35$ kc/s, $\chi_{bb}=235\pm63$ kc/s. Equation (**2**) similarly gives $\nu_0=10{,}919\cdot420\pm0\cdot001$ Mc/s, $(eqQ)_{OD}=353\pm4$ kc/s. Frequencies calculated from these parameters are listed in columns (*c*) and (*d*) respectively of Table 4.

It will be seen that equation (**1**) gives a somewhat better fit to the four strongest lines. However, the frequencies of unresolved components do not

show such good agreement, and synthesis of the absorption curve for the whole group of transitions shows that the use of equation (**1**) does in fact give the better fit. Further, the assumption of cylindrical symmetry gives, from Table **3**, $\chi_{aa}=154$ kc/s, $\chi_{bb}=22$ kc/s, and we cannot expect a very large deviation from these values.

Thus the best solution here is the simple one assuming symmetry about the bond axis ; $\nu_0=10{,}919\cdot420\pm0\cdot001$ Mc/s, $(eqQ)_{OD}=353\pm4$ kc/s. The absorption curve calculated from these parameters, using the frequencies of column (*d*)

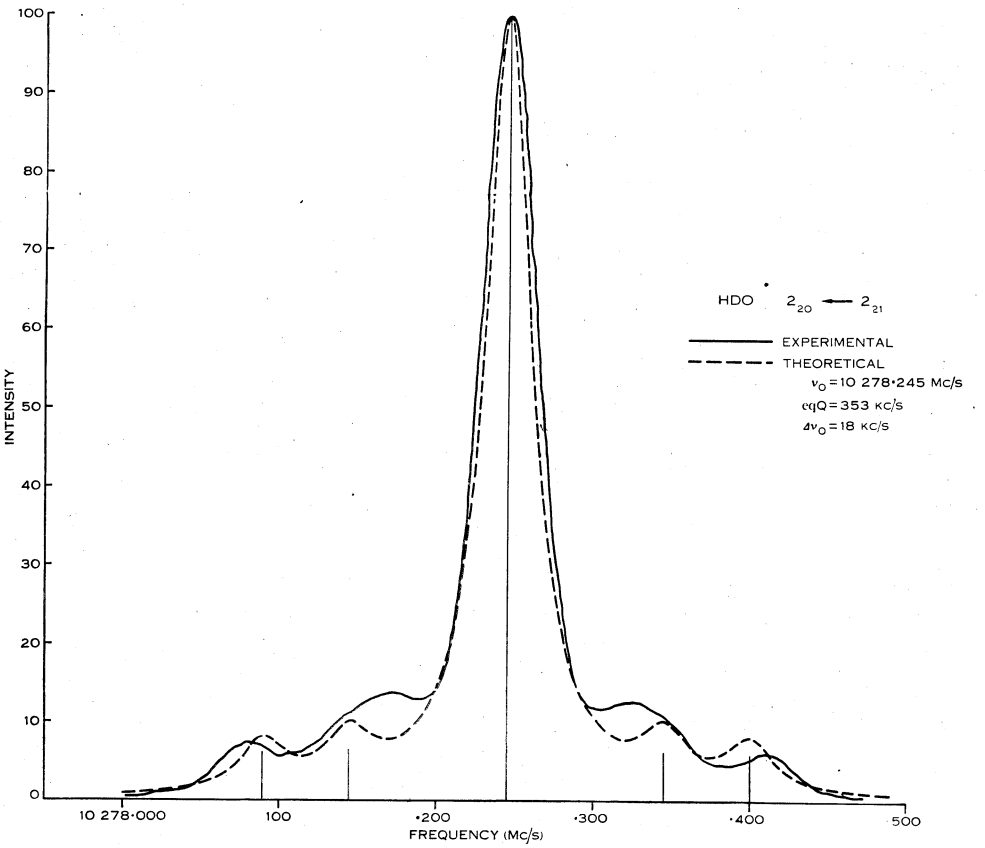

Fig. 7.—Calculated and observed spectra of HDO.

of Table 4, is shown in Figure 6. It is apparent that some discrepancy remains ; the lack of agreement is attributed to neglect of magnetic effects, to experimental error, and to use of an approximate line shape.

(*b*) *The HDO Spectrum*

With $(eqQ)_{OD}$ known approximately from the D_2O results, we can calculate up the HDO spectrum, using equation (**2**). From Figure 7, which compares the calculated and observed spectra, it is evident that the agreement is very poor, as regards both frequency and line shape. No significant improvement

is obtained by calculating $(eqQ)_{OD}$ from the peaks of the HDO spectrum, as is indicated in Table 5.

Since the discrepancies are well outside experimental error, it is reasonable to ascribe the lack of agreement to the neglect of magnetic effects, which are expected to be considerably larger in HDO than in D_2O. Accordingly, it may be assumed that the D_2O spectrum gives the best measure of the quadrupole coupling, and therefore to this approximation $(eqQ)_{OD} = +353 \pm 4$ kc/s, and $q_{OD} = \langle \partial^2 V / \partial \xi^2 \rangle = (1 \cdot 78 \pm 0 \cdot 02) \times 10^{15}$ e.s.u.

TABLE 5

HDO $2_{20} \leftarrow 2_{21}$ HYPERFINE STRUCTURE

Transition $F' \leftarrow F''$		Observed Frequency (Mc/s)*	Calculated Frequency (Mc/s) (a)†	(b)‡	Relative Intensity (Calculated)
2	1	10,278·081	10,278·090	10,278·099	12·1
2	3	·168	·145	·151	12·5
1	1	·245	·245	·245	36·2
2	2				55·8
3	3				100·0
3	2	·332	·345	·339	12·5
1	2	·411	·400	·391	12·1

* Approximate peak positions.

† For $\nu_0 = 10{,}278 \cdot 245$ Mc/s, $(eqQ)_{OD} = 353$ kc/s.

‡ For $\nu_0 = 10{,}278 \cdot 245$ Mc/s, $(eqQ)_{OD} = 333$ kc/s.

V. REFERENCES

BEARD, C. I., and BIANCO, D. R. (1952).—*J. Chem. Phys.* **20**: 1488–9.

BENEDICT, W. S., GAILAR, N., and PLYLER, E. K. (1956).—*J. Chem. Phys.* **24**: 1139–65.

BRODERSEN, S. (1953).—*J. Opt. Soc. Amer.* **43**: 1216–20.

HILSENRATH, J., *et al.* (1955).—Tables of thermal properties of gases. Circ. U.S. Bur. Stand. No. 564.

KOLSKY, H. G., PHIPPS, T. E., JR., RAMSEY, N. F., and SILSBEE, H. B. (1952).—*Phys. Rev.* **87**: 395–403.

LEE, C. A., FABRICAND, B. P., CARLSON, R. O., and RABI, I. I. (1953).—*Phys. Rev.* **91**: 1395–403.

OKAYA, A. (1956).—*J. Phys. Soc. Japan* **11**: 258–63.

POSENER, D. W. (1953).—M.I.T. Research Laboratory of Electronics Tech. Rep. No. 255.

POSENER, D. W., and STRANDBERG, M. W. P. (1954).—*Phys. Rev.* **95**: 374–84.

ROBINSON, G. W., and CORNWELL, C. D. (1953).—*J. Chem. Phys.* **21**: 1436–42.

SMITH, W. E. (1955).—*J. Opt. Soc. Amer.* **45**: 227–8.

STRANDBERG, M. W. P. (1949).—*J. Chem. Phys.* **17**: 901–4.

STRANDBERG, M. W. P. (1954).—"Microwave Spectroscopy." (Methuen: London.)

WEISBAUM, S., BEERS, Y., and HERRMANN, G. (1955).—*J. Chem. Phys.* **23**: 1601–5.

WHITE, R. L. (1955*a*).—*J. Chem. Phys.* **23**: 249–52.

WHITE, R. L. (1955*b*).—*J. Chem. Phys.* **23**: 253–5.

WHITE, R. L. (1955*c*).—*Rev. Mod. Phys.* **27**: 276–88.